Advanced Composites and Hybrid Materials (2022) 5:3068–3080
https://doi.org/10.1007/s42114-022-00558-4

ORIGINAL RESEARCH

Self-healing and polymer welding of soft and stiff epoxy thermosets via silanolates

Amelia A. Putnam-Neeb[1] · Jordan M. Kaiser[1,2] · Amber M. Hubbard[1] · Dayton P. Street[1] · Matthew B. Dickerson[1] · Dhriti Nepal[1] · Luke A. Baldwin[1]

Received: 18 February 2022 / Revised: 15 July 2022 / Accepted: 8 September 2022 / Published online: 23 September 2022

Abstract
Incorporating dynamic bonds into polymers enables static thermosets to be transformed into active materials, possessing the reprocessability of thermoplastics while maintaining the bulk properties of fully crosslinked networks. This new class of materials, termed covalent adaptable networks (CANs), has helped bridge the gap between traditional thermosets and thermoplastics. Here, epoxy-based adaptable networks were synthesized by combining a diepoxide monomer with an oligosiloxane prepolymer containing aminopropyl groups, which crosslink irreversibly, and silanolate end-groups, which participate in dynamic bonding. Two separate diepoxide crosslinkers were used to give a range of soft to stiff materials with a Young's modulus varying from 12 MPa to 2.2 GPa. This study documents how the thermal and mechanical properties (e.g., glass transition temperature and modulus) are affected by compositional changes in these silanolate networks. Dynamic bonding also results in self-healing properties, offering the ability to repair structural polymers and composites. When combined with tunable mechanical properties, self-healing capabilities make these materials well-suited to be sustainable alternatives for many traditional thermosets. For example, we demonstrated the ability to weld a stiff epoxy thermoset to a dissimilar soft material, a feature traditional epoxies do not permit.

Keywords Silanolate · Covalent adaptable networks · Self-healing · Epoxy · Thermosets · Polymer welding

1 Introduction

Synthetic polymers are ubiquitous in modern society due to the low cost and ease of processing [1, 2]. In an effort to improve functionality, novel polymer-based materials are continually being developed to support a range of industries such as packaging [3], energy [4, 5], remediation [6, 7], biomedical [8–10], military [11], and automotive [12]. The increasing diversity of macromolecules has allowed for the development of hybrid systems; however, thermoplastics and thermosets remain the most common classes of polymeric materials. Thermoplastics rely on polymer chain entanglements for bulk structure and can therefore be melted, deformed, and reprocessed in the molten state, resulting in recyclable plastics for sustainability. This characteristic, however, leads to poor suitability for applications that require high thermal, chemical, and structural stability. Thermosets, on the other hand, possess permanent, rigid networks that provide strength and durability but lack reprocessing capabilities [13]. While thermosets have ideal mechanical properties due to highly crosslinked networks, only thermoplastics have traditionally been able to offer reprocessability. The push towards multi-functional materials and sustainability has led to the search for viable alternatives that can combine the robust mechanical properties of a thermoset with the reprocessing capabilities of a thermoplastic.

Covalent adaptable networks (CANs) are promising candidates to integrate the desirable properties of both polymer types. This class of polymers incorporates dynamic covalent bonds for reversible crosslinking, leading to thermosets with self-healing properties [14–18]. This feature can provide reprocessability or recycling of thermosets, giving more sustainable options for various applications by increasing the lifetime of polymer components [2, 19–21]. Dynamic

✉ Luke A. Baldwin
luke.baldwin.1@us.af.mil

[1] Air Force Research Laboratory, Wright Patterson Air Force Base, Dayton, OH 45433, USA

[2] UES, Inc, Dayton, OH 45432, USA

bonding can allow self-healing of soft, pliable polymers such as vibration damping parts, seals, or medical devices, which all commonly fail over a long-term service life [22–25]. Bond exchange reactions can also heal microcracks or fractures that would typically render a structural or load-bearing part inoperative. Furthermore, dynamic bonding supports the recyclability of these parts once they do reach the end of their service life. But, in addition to sustainability, adaptable networks can also facilitate welding of thermosets through bond exchanges at the interface [26–28]. Although polymer welding is typically limited to suitable thermoplastics, incorporating compatible dynamic chemistry into different thermosets can enable strong bonding between the dissimilar materials [29, 30]. In the case of welding soft and stiff materials together, the healing capability can help prevent delamination caused by disparate mechanical properties, allowing different thermoset materials to work together seamlessly.

To prepare adaptable networks with a range of moduli for welding dissimilar thermosets, the materials should be comprised of both soft and stiff components to effectively tune the mechanical properties. Polysiloxanes are commonly used in applications for soft materials like medical devices and soft robotics [31, 32] due to excellent chemical compatibility and low toxicity. Because of these properties, several methods to imbue self-healing behavior into static siloxanes have been pursued [23–25, 31, 33–35]. Previous adaptable networks have been developed by incorporating basic species for ring opening of cyclic siloxanes [23, 33] or after polymerization of silanes [36]. This reaction installs silanolate end groups onto polymer chains, which can then react with other siloxanes for dynamic bond exchanges. The resulting adaptable networks have low glass transition temperatures (T_g) and moduli, giving a self-healing elastomer. Though many silicones are soft and flexible, recent work has also used siloxane equilibration for dynamic bonding within a stiff epoxy thermoset [36]. The silanolate-terminated siloxane oligomer contained aminopropyl side chains to crosslink with a diepoxide monomer yielding a stiff epoxy thermoset (e.g., T_g of 83 °C and Young's modulus of 2.2 GPa) with good recyclability and self-healing capabilities [36]. However, using polysiloxanes in stiff adaptable networks still remains relatively underexplored.

The work presented here focuses on siloxane/epoxy adaptable networks with tunable mechanical properties by pairing dynamic components with contrasting monomers to give materials with a range of moduli. Herein, we build on a previous report that employs a poly(3-aminopropyldimethoxymethylsilane) oligomer (KPAMS) as the precursor for the dynamic component within the epoxy thermosets [36]. We systematically studied different diepoxide crosslinkers (Fig. 1) to give contrasting mechanical properties. A flexible crosslinker, 1,4-butanediol diglycidyl ether (BDDE), was used to give a soft material, and diglycidyl ether bisphenol A (DGEBA) was used as a rigid monomer for stiff thermosets. For both chemistries, the ratio of starting materials was varied to study the thermal, mechanical, and self-healing properties as a function of the crosslinker concentration. Furthermore, we also demonstrated that polymer welding can be accomplished with fully cured thermoset networks. This provides evidence that soft and stiff thermosets comprising dynamic motifs can be used to create complex architectures instead of relying on conventional thermoplastics. With this work, we show that a wide range of thermomechanical properties can be achieved for dynamic thermosets solely based on chemical variations. This capability allows sustainable self-healing materials that can be pliant or stiff for various applications such as vibration dampening pads or structural adhesives, respectively. Additionally, this tunability also enables easier recycling options downstream by avoiding the traditional composite approach.

2 Experimental

2.1 Materials

Potassium hydroxide (KOH), 3-aminopropyldimethoxymethylsilane (AMS), and 2,2-bis(4-glycidyloxyphenyl)propane (DGEBA) were purchased from TCI America. 1,4-Butanediol diglycidyl ether technical grade (BDDE) was purchased from Sigma Aldrich. Acetone was purchased from Fisher Scientific. All chemicals were used as received.

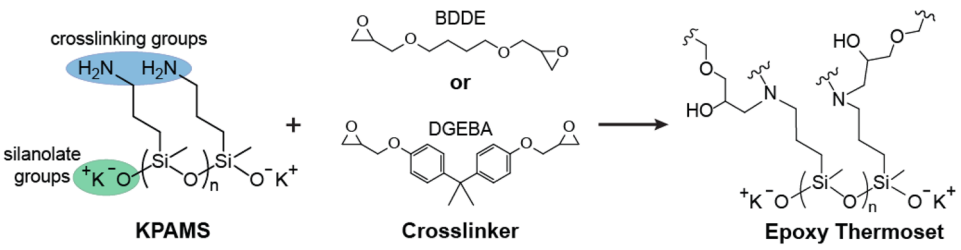

Fig. 1 Synthesis of silanolate adaptable networks. Either DGEBA (rigid) or BDDE (flexible) crosslinker was added to the oligosiloxane prepolymer (KPAMS) at 40, 60, or 80 wt% to synthesize the adaptable networks with a range of moduli. The epoxide groups of the crosslinker react with the amines on the KPAMS backbone to give an epoxy thermoset containing silanolate groups for dynamic bonding

2.2 Synthesis of KPAMS

2.2.1 PAMS

Oligoaminopropylmethylsiloxanediolate (PAMS) was synthesized in continuous flow using a Vapourtec R-Series modular flow chemistry system. The flow system was equipped with R2 C+ piston pumps and a stainless steel, high-temperature tube reactor. The PAMS was synthesized by reacting 25 mL of deionized water (1.39 mol) with 100 mL AMS (0.58 mol) at 160 °C with a residence time of 60 min. Once the product was collected, byproducts and excess water were removed via rotary evaporation to yield a colorless, viscous solution (69.7 g). Residence time and temperature were chosen based on analysis by matrix-assisted laser desorption ionization time-of-flight (MALDI-TOF) mass spectrometry using a cyano-4-hydroxycinnamic acid (HCCA) matrix to determine molecular weight in comparison to polymers produced via batch reaction (Fig. S1).

2.2.2 KPAMS

The potassium silanolate derivative of PAMS, or KPAMS (bis(potassium) oligoaminopropylmethylsiloxanediolate), was synthesized based on a previously reported procedure [36]. For this study, potassium hydroxide content was held constant at 5 wt%. For synthesis, PAMS and 5 wt% KOH were mixed in a round-bottom flask at 90 °C for 4 h. Byproducts were then removed via rotary evaporation to yield a viscous, slightly cloudy solution. Characterization by nuclear magnetic resonance (NMR) spectroscopy of PAMS compared to KPAMS is shown in Fig. S2. ^{1}H NMR spectra was obtained using a Bruker Avance 400 MHz spectrometer in deuterated dimethyl sulfoxide (DMSO-d_6) solvent. PAMS: ^{1}H NMR (DMSO-d_6, 400 MHz)—δ 1.92 (s, 5H), 1.46–1.32 (m, 4H), 0.54–0.39 (m, 4H), 0.06 (s, 4H). KPAMS: ^{1}H NMR (DMSO-d_6, 400 MHz)—δ 1.42 (q, 2H), 0.52 (m, 1H), 0.51–0.29 (m, 1H), 0.10 (m, 2H), −0.00 to −0.14 (m, 1H).

2.3 Synthesis of thermoset networks

2.3.1 KPAMS-BDDE

Cured samples for thermal and mechanical analysis were prepared by combining KPAMS and BDDE monomer in the specified ratio. The BDDE monomer was degassed by stirring under vacuum (~100 torr) for 1 h prior to synthesis. After degassing, the two monomers were combined and stirred under vacuum for 15 min. The reaction mixture was then poured into a polytetrafluoroethylene (PTFE) mold which was preheated in an oven for 20 min at 80 ℃. The PTFE molds were machined to specific dimensions required for thermal or mechanical testing, which will be discussed in the corresponding characterization methods sections. After pour casting, the samples were cured in a two-step process (1 h at 80 ℃ and 2 h at 110 ℃) and removed from the PTFE molds after cooling to ambient temperatures.

2.3.2 KPAMS-DGEBA

To synthesize KPAMS-DGEBA samples, DGEBA was first degassed for 1 h by heating to 80 ℃ and stirring while under vacuum (~100 torr). Once the DGEBA was weighed out in the reaction vessel, 4 wt% acetone (w.r.t. total reaction weight) was added. The DGEBA and acetone were stirred for 5 min to mix before KPAMS was added to the vial. The mixture was then stirred under vacuum for 15 min to remove acetone and potential air bubbles. After mixing, the white KPAMS-DGEBA blend was poured into preheated PTFE molds (80 ℃), which were then cured at 80 ℃ for 1 h and 110 ℃ for 2 h. Samples were cooled to room temperature before removal from the PTFE molds. To mitigate the formation of air bubbles, the 40 wt% DGEBA formulation was mixed without acetone addition.

2.4 Characterization

Stoichiometric ratios of amine and epoxide groups in each of the adaptable networks were calculated using ^{1}H NMR spectra of the starting materials with an internal standard. Similar amounts (~25 mg) of the monomer and the standard (mesitylene) were dissolved in DMSO-d_6 (1 g) to be analyzed by ^{1}H NMR spectroscopy. From the resulting spectra, chosen peaks were integrated based on the standard reference peak. Aminopropyl –CH_2– group peaks were used to calculate –NH_2 content in KPAMS, and proton peaks from epoxide groups were used for diepoxide monomers. Peaks were integrated to calculate millimole of functional group per gram of monomer, which was then used to calculate the stoichiometric ratio of amines and epoxides for each adaptable network formulation.

In situ Fourier transform infrared (FT-IR) spectroscopy was performed using a Thermo Nicolet 6700 FT-IR equipped with a Simplex Scientific heated stage. For each adaptable network synthesis, the two monomers were mixed together for 10 min before the reaction mixture was compressed between two NaCl salt disks. The salt disks with the reaction mixture were placed in a heated stage within the FT-IR instrument and then programmed to heat with a typical curing cycle of 80 ℃ for 1 h and 110 ℃ for 2 h.

2.4.1 Material characterization

Thermogravimetric analysis (TGA) of the epoxy networks was performed on a TA Instruments TGA Q500.

Experiments consisted of a temperature ramp from room temperature to 800 °C at a heating rate of 10 °C min^{-1} under a nitrogen environment to avoid oxidative thermal degradation. The temperature of decomposition at 5 wt% mass loss for all materials was extracted from the TGA curves (Figs. S3 and S4) to determine thermal stability. These values were taken as the maximum operating temperature for further characterization. To show water removal from the materials, cyclic TGA experiments (Fig. S5) were conducted by performing TGA up to 200 °C and then repeating the test using the same sample. The final mass loss at the end of each cycle is reported in Table S1.

Each of the adaptable networks were analyzed by differential scanning calorimetry (DSC) using a TA Instruments Discovery DSC 2500. While under a nitrogen environment, samples were ramped from −50 to 150 °C for two cycles at a ramp rate of 5 °C min^{-1}. The samples were equilibrated for 2 min between heating and cooling. The glass transition temperature (T_g) was collected as the inflection point of the second heating cycle.

A Discovery DMA 850 (TA Instruments) was used for all dynamic mechanical analysis (DMA) and stress relaxation studies in tension mode. Samples of each of the materials were cast in PTFE molds ($l \times w \times h$: 20 mm × 6 mm × 1 mm) and cut to a width of 2 mm prior to testing. Storage modulus (E') and loss factor curves, or tan δ, were obtained with an axial dynamic strain of 0.1% and a frequency of 1.0 Hz. The chosen strain was based on a strain-sweep to determine the region of linear response where E' was constant prior to testing. Oscillation temperature ramp studies of KPAMS-BDDE samples were performed from −30 to 100 °C at 5 °C min^{-1}, and KPAMS-DGEBA samples were tested from −10 to 150 °C at 5 °C min^{-1}. Temperature ranges were chosen to ensure the E' was recorded well into the rubbery regime as a means to calculate the molecular weight between crosslinks and to avoid instrument limitations. Glass transition temperatures were recorded as the onset of the drop in E' and the peak of the tan δ curve.

Molecular weight between crosslinks (M_c) and crosslinking density (v_c) was calculated as Eq. 1 [36–38],

$$E' = 3RTv_c = \frac{3RT\rho}{M_c} \quad (1)$$

where E' is the storage modulus at T_g+50 °C, R is the universal gas constant, T is the absolute temperature at T_g+50 °C, and ρ is the calculated density of the material. For KPAMS-DGEBA materials, the M_c was calculated based on the highest T_g. For the 60 wt% DGEBA formulation, the E' was taken at T_g+ 80 °C to ensure the material was well within the rubbery regime.

Isothermal stress relaxation experiments were performed using an axial strain of 1.0% over a relaxation time of 50 min. The samples were equilibrated to the testing temperature of 110 °C for 5 min prior to testing. Measured stress was normalized for comparison.

Soxhlet extraction was used to remove any uncured starting materials by extracting with refluxing acetone for 24 h. The insoluble portion of the sample was then dried in an oven overnight at 80 °C. The gel fraction was calculated by dividing the weight of the dried, insoluble sample by the initial sample weight.

2.5 Tensile testing

Mechanical properties of all thermoset materials were evaluated by tensile testing of dogbone specimens. The test specimens were prepared after synthesis by casting in PTFE molds to dimensions following the ASTM D638 Type V standard [39]. The resulting dogbones were 63-mm long overall, with the bridge having dimensions of 10 mm × 3 mm × 4 mm ($l \times w \times h$). The KPAMS-DGEBA formulations were tested with an MTS Insight 5 kN Material Testing System equipped with a 2.5 kN load cell. Softer samples were tested using pneumatic grips with a pressure of 40 psi. Stiff materials were held in hand-tightened mechanical grips to prevent slipping. The KPAMS-BDDE samples were tested using an ADMET Planar Biaxial Testing System with a 50 lbf load cell and self-tightening grips, with the exception of self-healing samples, which were also tested with the MTS Insight. All tensile tests were performed with a crosshead speed of 2 mm min^{-1}. Modulus values were taken as the initial slope of the resulting stress–strain curves. Toughness was calculated as area under the stress–strain curve. Error is reported as one standard deviation.

2.6 Self-healing and polymer welding

Self-healing properties of the adaptable networks were evaluated by welding together fractured dogbone specimens. Healing conditions were chosen for consistency between both soft and stiff materials so polymer welding of different thermosets could be performed using the same parameters. The dogbone pieces were positioned in a 3-piece aluminum mold (Fig. S6) and pressed together using a 30 ton WABASH Hot Press. As Fig. S6 shows, the mold containing samples was placed on the heated platen (110 °C) for 15 min to equilibrate before compressing for 45 min at 5 MPa. After welding, the mold was allowed to cool before removing the samples. Tensile tests of the self-healed dogbone specimens were performed to compare the mechanical properties of the pristine and healed samples. Polymer welding was demonstrated using the same parameters.

3 Results and discussion

To make soft and stiff epoxy adaptable networks, a diepoxide monomer was combined with a polysiloxane prepolymer, and curing occurred by epoxy groups reacting with the amines on the oligomer backbone. Once cured, siloxane equilibration offered dynamic bond exchange reactions within the thermoset, as depicted in Fig. S7. Two different diepoxides shown in Fig. 1 were tested as crosslinkers to investigate the versatility of silanolate adaptable networks. Diglycidyl ether bisphenol A (DGEBA) was used to make a stiff epoxy network, and 1,4-butanediol diglycidyl ether (BDDE) was used to produce a soft, ductile material. To evaluate how compositional ratios can impact material performance, the epoxy crosslinking groups were added to the polysiloxane in three different ratios of 40%, 60%, or 80% by weight of the diepoxide monomer. These formulations were chosen for each epoxy crosslinker to yield a solid resin with dynamic bonds. Formulations outside this range did not have enough crosslinking to yield a workable epoxy network.

Prior to making the adaptable networks, the polysiloxane prepolymer was prepared through the polymerization of 3-aminopropyldimethoxymethylsilane (AMS). For this reaction, AMS was oligomerized by combining with deionized water in continuous flow to yield oligoaminopropylmethylsiloxanediolate (PAMS), as shown in Fig. 2. A continuous flow system was used for automation and ease of synthesis in comparison to previous batch reaction methods [36]. Since flow chemistry often provides several advantages over traditional batch protocols (e.g., improved mixing, heat transfer, and scale-up [40–42]), this method was chosen to increase production due to the large material quantities needed for mechanical testing. This continuous approach resulted in more efficient and scalable synthesis of PAMS, with a production rate of 5.6 g hr^{-1}. For comparison, AMS was consumed at a rate of 7.6 g hr^{-1} in flow compared to 2.3 g hr^{-1} in batch.

Once PAMS was synthesized, the oligomer was then functionalized with silanolate end groups to facilitate dynamic bond exchanges. Potassium hydroxide (5 wt%) was added to the PAMS to make bis(potassium) oligoaminopropylmethylsiloxanediolate (KPAMS). The addition of KOH decreased the molecular weight from 1500–2000 (PAMS, n=11–19) to 900–1500 g mol^{-1} (KPAMS, n=7–15) as the base reacted with the polysiloxanes to shorten the oligomer chains and give silanolate end groups. The KOH was added at 5 wt% to give optimal stress relaxation of the epoxy network. Preliminary results demonstrated that lower concentrations provided insufficient dynamic bond exchanges, while higher concentrations required high temperatures for self-healing to occur. Prior work has shown that high KOH concentrations lead to increased glass transition temperatures due to the strong ionic interactions of potassium silanolate groups [36]. To maintain a workable glass transition temperature for self-healing and welding of the materials, 5 wt% KOH was used to synthesize KPAMS for all adaptable network formulations.

3.1 KPAMS-BDDE (soft)

To synthesize the soft epoxy adaptable network, BDDE was used as the crosslinker (Fig. 1), which incorporates a short carbon chain for flexibility. This monomer was chosen because it is commercially available and widely used as a crosslinker for soft materials, such as hyaluronic acid dermal fillers [43] or dextran polymers [44]. The BDDE was mixed with KPAMS at 40 wt%, 60 wt%, or 80 wt% prior to pour casting. Combining two flexible starting materials, including the carbon chain diepoxide and silicone hardener, provided malleable thermosets for all three of the KPAMS-BDDE formulations tested. Thermal stability of the cured resins was investigated using TGA (Fig. S3). The decomposition temperature at 5% mass loss (T_d) increased with a higher content of BDDE (Table S2), from 222 °C at 40 wt% to 343 °C at 80 wt%.

For each formulation, glass transition temperatures (T_g) were obtained from DSC and confirmed by DMA, as recorded from both E' and tan δ curves (Table S2). While both 40 wt% and 80 wt% BDDE formulations produced similar T_g values at −7 °C, interestingly, the T_g of 60 wt% BDDE

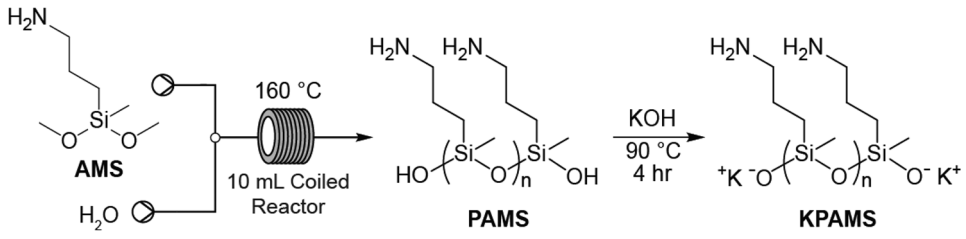

Fig. 2 Synthesis of bis(potassium) oligoaminopropylmethylsiloxanediolate (KPAMS) from 3-aminopropyldimethoxymethylsilane (AMS). Continuous flow chemistry was used to oligomerize AMS to produce PAMS. The oligomer was then reacted with KOH to give silanolate end groups for dynamic bonding

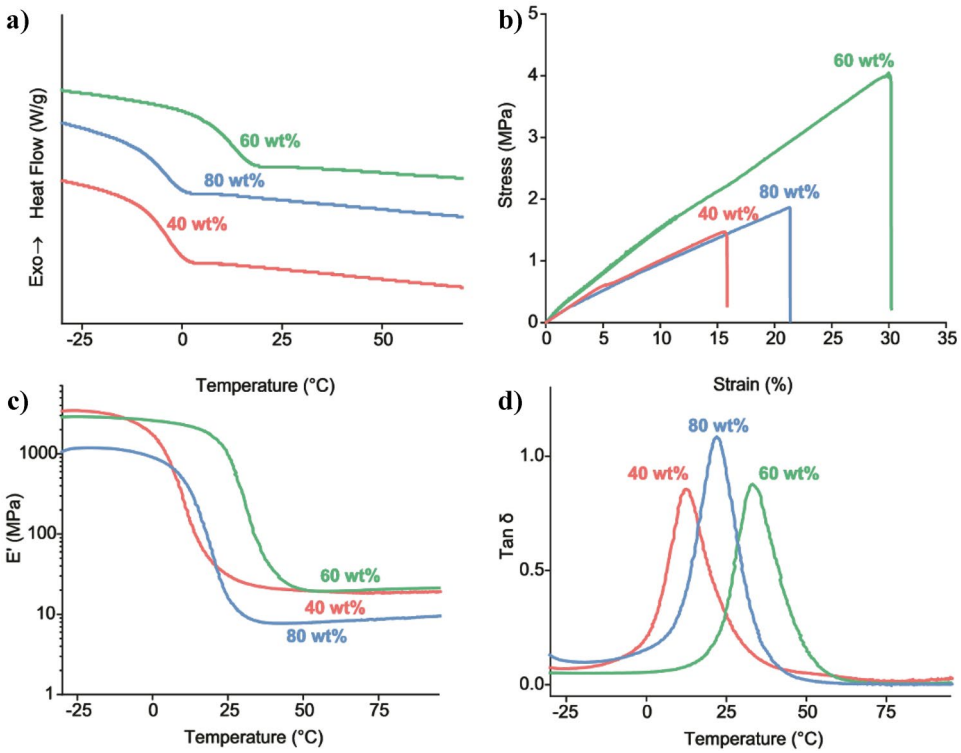

Fig. 3 Representative characterization data of KPAMS-BDDE materials, including **a** DSC, **b** stress–strain curves from tensile testing, and **c** storage modulus and **d** tan δ curves obtained from DMA. Both DSC and DMA showed that 60 wt% BDDE had a higher T_g than the other two formulations. The improved mechanical properties from 60 wt% BDDE indicate an optimal ratio between the two starting materials

was noticeably higher at 11 °C (cf., Fig. 3a). For comparison, note that a crosslinked polydimethylsiloxane adaptable network with tetramethylammonium silanolates for dynamic bonding has a T_g of −129.5 °C and a Young's modulus of 0.389 MPa [23], similar to a silicone elastomer. While each of the KPAMS-BDDE formulations are soft materials, these epoxy networks have thermal and mechanical properties in between traditional silicones and epoxies.

In addition to higher T_g values, the 60 wt% BDDE also had improved mechanical properties in comparison to the other formulations. Table 1 shows that Young's modulus (18 MPa), toughness (600 kJ m^{-3}), tensile strength (3.9 MPa), and strain at break (29%) were all highest for the 60 wt% formulation. In other words, in all thermal and mechanical aspects, 60 wt% BDDE appears to be the optimal concentration. This is evidenced by the highest performing mechanical properties in tensile tests (i.e., modulus and toughness) as well as the highest T_g in DMA and DSC. However, it is worth considering the tensile tests and DMA results in tandem. All tensile testing was performed at ambient conditions (~25 °C), where both the 40 wt% and 80 wt% formulations were within the rubbery regime. However, the 60 wt% was in transition from the glassy to rubbery region, indicating that a direct comparison of mechanical properties from structure/property relationships may be difficult. These modulus values and trends are confirmed by comparing the tensile tests and DMA results.

To elucidate these trends, we report the molecular weight between crosslinks (M_c) as seen in Eq. 1 and numerically reported in Table 1. These results validate the observed trend in thermal and mechanical properties. The crosslink density (v_c), which is inversely proportional to M_c, increases with improved modulus and T_g, as expected [45–47]. Therefore, the increased stiffness and T_g with 60 wt% BDDE is due to the higher degree of crosslinking within the adaptable network.

To explain why the 60 wt% formulation gives an optimal balance between the dynamic oligosiloxane component and the diepoxide crosslinker, the stoichiometric ratios of amine to epoxide groups were calculated via ^{1}H NMR. The results in Table S3 show that 60 wt% BDDE gives almost

Table 1 Mechanical properties and crosslinking density of KPAMS-BDDE networks

BDDE content	Young's Modulus (MPa)	Toughness (kJ m^{-3})	Tensile Strength (MPa)	Elongation at Break (%)	M_c (kg mol^{-1})	v_c (mol m^{-3})
40 wt%	12.4 ± 0.3	120 ± 10	1.4 ± 0.1	15 ± 1	0.61 ± 0.05	1900 ± 100
60 wt%	18 ± 2	600 ± 100	3.9 ± 0.5	29 ± 2	0.47 ± 0.03	2400 ± 100
80 wt%	11.5 ± 0.6	210 ± 30	1.8 ± 0.2	21 ± 1	1.13 ± 0.01	1040 ± 10

a 2:1 ratio of epoxide to amine groups. Epoxy thermosets generally use a 1:1 stoichiometric ratio, but a slight excess of amines ensures complete reaction of epoxides [48]. Here, the aminopropyl groups from KPAMS contain 1° amines, which are converted to 2° amines upon reaction with epoxides. With a higher ratio of epoxide groups, any epoxides remaining after 1° amines are consumed can then react with the 2° amines. Therefore, two epoxide groups can react with each $–NH_2$, meaning a stoichiometric balance is achieved at the 2:1 ratio seen with 60 wt% BDDE. Even with this ratio, the epoxide groups were exhausted quickly with 60 wt% BDDE, as observed from in situ FT-IR in Fig. S8a. With 40 wt% BDDE, an excess of amines contributes to lower T_g and v_c [48], as well as Young's modulus and tensile strength [49]. At 80 wt%, epoxides outnumbered amine groups 5.4:1, limiting the amount of crosslinking within the network. For both 40 and 80 wt% BDDE, a limited amount of one monomer restricts crosslinking within the network. Since both KPAMS and BDDE have flexible structures, neither influence bulk mechanical properties strongly. Rather, the mechanical properties are dictated primarily by the degree of crosslinking, which is optimized in the middle formulation with a more balanced ratio of starting materials.

3.2 KPAMS-DGEBA (stiff)

For the stiff adaptable network, DGEBA was chosen as a crosslinking agent for KPAMS because it is commercially available and commonly used as a starting material to make stiff epoxy thermosets [50]. For synthesis, the viscous DGEBA starting material typically required the addition of a small amount of acetone to aid in mixing. However, thermal and mechanical characterization still showed signs of limited miscibility between the two starting materials, which will be discussed later.

For the cured thermoset, TGA data followed a similar trend as KPAMS-BDDE, with increasing T_d from higher crosslinker concentrations (Fig. S4). The DGEBA materials generally had lower thermal stability than BDDE, with a range from 138 to 289 °C (Table S4). However, KPAMS-DGEBA also had a lower crosslink density, contributing to the reduced thermal stability. Comparing materials with a similar v_c, such as 60 wt% BDDE (T_d ~253 °C) and 80 wt% DGEBA, (T_d ~289 °C) gives the expected result of more thermal stability from DGEBA. Additionally, cyclic TGA experiments (Fig. S5) indicated some water loss during testing. Table S1 shows that the final mass loss for the second TGA cycle is lower for KPAMS-DGEBA materials after the water was removed during the first temperature ramp. This result suggests that the observed decomposition temperature at 5% mass loss may in part be due to residual water coming from the synthesis of KPAMS.

Variations in crosslink densities from KPAMS-BDDE to KPAMS-DGEBA networks can be attributed to differences in stoichiometry of reactive groups. Since DGEBA has a higher molecular weight than BDDE, the stoichiometric ratios of the networks, which were formulated by weight, deviated from what was seen in the KPAMS-BDDE materials. Table S5 shows that, similar to KPAMS-BDDE, 80 wt% DGEBA still gives an excess of epoxides, and the surplus of amine groups with 40 wt% contributes to lower T_g, v_c, and mechanical properties [48, 49]. For 60 wt% DGEBA, there is a slight excess of epoxides, but still below the 2:1 ratio where all amines are consumed fully. In situ FT-IR of 60 wt% DGEBA (Fig. S8b) shows that the epoxides are eventually reacted away, albeit slower than for KPAMS-BDDE because of the rigid structure of DGEBA.

The cured KPAMS-DGEBA adaptable networks showed a direct correlation between stiffness and DGEBA concentration. Young's modulus (Table 2) increased by almost two orders of magnitude from 35 MPa to 2.5 GPa between the lowest and highest concentrations of DGEBA. The stress–strain curves in Fig. 4b show that the soft, flexible 40 wt% DGEBA had a considerable strain at break (32%) but low tensile strength (4.6 MPa) while the stiff 80 wt% DGEBA was brittle (2.4% strain at break) with a high tensile strength (51 MPa). This trend makes sense as the addition of the rigid DGEBA monomer reduces chain flexibility, leading to higher T_g and increased mechanical performance. By simply altering the KPAMS to DGEBA ratio, we can achieve tunable mechanical properties without altering the thermoset chemistry.

Along with the change in stiffness, both DSC and DMA confirmed a substantial increase in T_g with more diepoxide crosslinker. Figure 4a shows T_g values increased from 6 to 92 °C between 40 and 80 wt% DGEBA, respectively. Similar to KPAMS-BDDE networks, the crosslink density

Table 2 Mechanical properties and crosslinking density of KPAMS-DGEBA networks

DGEBA content	Young's Modulus (MPa)	Toughness (kJ m^{-3})	Tensile Strength (MPa)	Elongation at Break (%)	M_c (kg mol^{-1})	v_c (mol m^{-3})
40 wt%	35 ± 8	900 ± 100	4.6 ± 0.5	32 ± 3	1.5 ± 0.1	760 ± 80
60 wt%	1130 ± 20	500 ± 100	23.9 ± 0.5	3.5 ± 0.4	0.9 ± 0.2	1200 ± 300
80 wt%	2500 ± 100	700 ± 200	51 ± 5	2.4 ± 0.4	0.47 ± 0.02	2300 ± 100

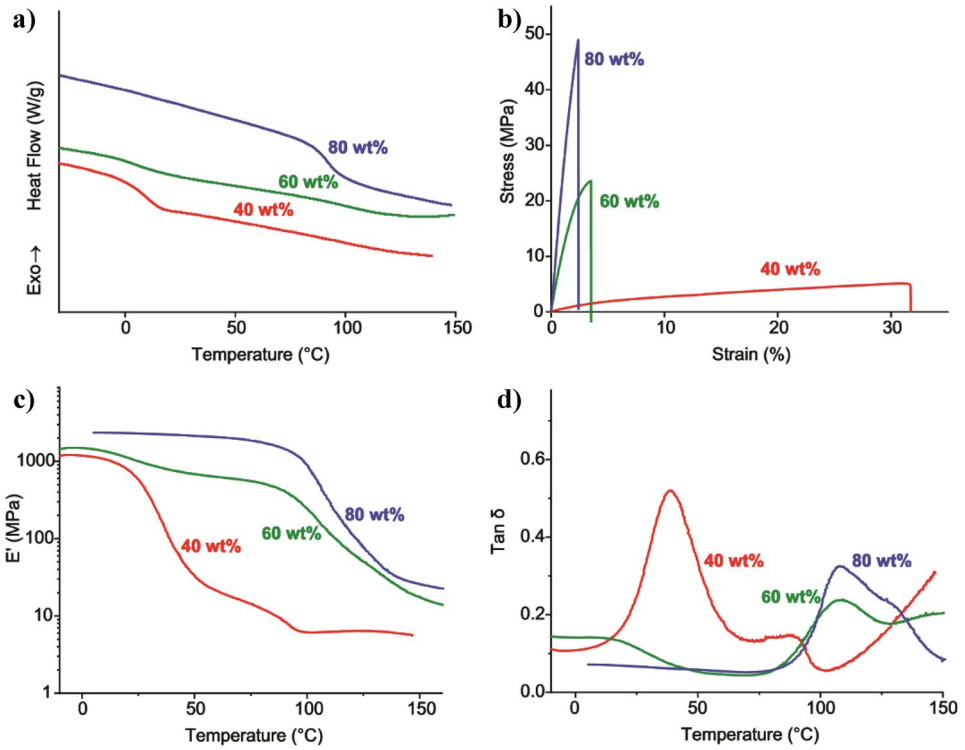

Fig. 4 Representative characterization data for each formulation of KPAMS-DGEBA adaptable networks, including **a** DSC, **b** stress–strain, **c** storage modulus, and **d** tan δ curves. Observed T_g values from both DSC and DMA increased with more DGEBA crosslinker. Tensile testing also showed vastly different mechanical properties between the three formulations, with higher concentrations of the rigid DGEBA monomer leading to an increase in stiffness

correlated with both stiffness and T_g. The M_c dropped and v_c increased with more DGEBA (Table 2). Although the BDDE monomer exhibited optimal performance at 60 wt%, the degree of crosslinking and the material properties for the DGEBA-crosslinked networks had a monotonic relationship. In contrast to the flexible BDDE, the rigid structure of DGEBA directly contributes to the mechanical properties of the KPAMS-DGEBA thermosets.

Table 2 shows little difference in toughness between the three formulations. The 60 wt% DGEBA material gives about half the strength of 80 wt% without a significant increase in ductility (Fig. 4b). Although a low modulus polysiloxane is added to DGEBA here, it does not contribute ductility to increase toughness. Most epoxy resins incorporating DGEBA typically become brittle with a high degree of crosslinking [51], and fillers or toughening agents are often dispersed throughout the epoxy resin to moderate brittleness and increase toughness. Elastomers such as butadiene-acrylonitrile are commonly used for rubber-toughened epoxies [52], although many other polymers like polyether sulfones [53–55], polyether imides [56–59], acrylics [60], polyurethanes [61], and polysiloxanes [62, 63] have been studied as organic modifiers for improving mechanical properties. The limited toughness from the 60 wt% DGEBA formulation here suggests that the KPAMS may not be fully compatible with the DGEBA. Rather than the low modulus component distributing stress throughout the bulk material, poor mixing between KPAMS and DGEBA could be leading to regions of differing compositions. As a result, bulk mechanical properties would be limited by interactions between the different regions.

To confirm immiscibility of the starting materials, a PAMS-DGEBA control with no dynamic component was compared to the silanolate-containing KPAMS-DGEBA counterpart. Both materials had 60 wt% DGEBA, but the control with PAMS, the precursor to KPAMS, did not have silanolates for dynamic bonding. Analysis of the two materials by DSC and DMA in Fig. S9 shows that without the silanolate group, the PAMS polysiloxane was more evenly distributed throughout the material, leading to a single observed T_g at ~75 °C. Upon the addition of potassium silanolate, two T_g's were present, suggesting poor mixing between the KPAMS and DGEBA [63]. The reduced miscibility between the two starting materials gives a low T_g (4 °C) from the polysiloxane-rich component and a high T_g (103 °C) from the DGEBA-rich component. This phenomenon is also visible in the DMA of each formulation (Fig. 4c and d). As reported in Table S4, two T_g's were present with both 40 wt% and 60 wt% DGEBA materials. For the 80 wt% formulation, with more crosslinker present and consequently less silanolate, the system is dominated by DGEBA characteristics, so a second T_g from the polysiloxane is not evident. Overall, these results provide evidence that the ionic nature of silanolates may be influencing the limited miscibility between the two starting materials. Future investigations include prediction and control of these interactions with distinct chemical moieties and counterions.

3.3 Polymer welding of dissimilar materials

3.3.1 Stress relaxation

Stress relaxation experiments were used to evaluate the dynamic bonding for both KPAMS-BDDE and KPAMS-DGEBA adaptable networks to determine efficacy for self-healing and polymer welding. The studies in Fig. 5a and b indicate that in both materials, more KPAMS (i.e., less diepoxide crosslinker) leads to faster relaxation. This trend is perfectly reasonable, as increasing the KPAMS component increases the number of dynamic bond exchange reactions occurring per unit time and volume. Control experiments in Fig. 5c and d confirm that incorporating the dynamic bond exchanges from potassium silanolate in KPAMS is contributing to relaxation. For both networks, the formulations with 60 wt% diepoxide monomer were compared to the same material using PAMS instead of KPAMS. Figure 5c shows that PAMS-BDDE, which lacks dynamic bonding, is not able to appreciably relax stress. However, the KPAMS derivative with silanolate groups relaxes stress through siloxane equilibration. In Fig. 5d, the PAMS-DGEBA thermoset does exhibit some inherent polymer network rearrangement, but the adaptable network with KPAMS is able to relax the applied stress. These results show that both KPAMS-BDDE and KPAMS-DGEBA exhibited potential for self-healing through bond exchange reactions.

For comparison, all stress relaxation experiments were performed at 110 °C, which was chosen as the welding temperature to exceed the T_g of both soft and stiff samples. This temperature was well above the T_g of the soft KPAMS-BDDE materials, leading to fast relaxation for high loadings of silanolate (Fig. 5a). For stiff materials, longer times were required to relax stress fully (Fig. 5b). The 40 wt% and 60 wt% formulations of both materials showed dynamic bonding to appreciably relax stress within 45 min, which was therefore used for self-healing and welding.

3.3.2 Self-healing

Based on stress relaxation results, self-healing properties of the materials were evaluated by healing all samples at 110 °C for 45 min under 5 MPa of pressure. These parameters were based on conditions suitable for both soft and stiff materials to provide a direct comparison between the two. Self-healing was assessed by healing fractured dogbone specimens and comparing tensile tests with the pristine samples. Figure 6 shows stress–strain curves of both soft and stiff adaptable networks.

Given the optimal properties of the 60 wt% BDDE adaptable network, self-healing of the soft material was investigated using that formulation. As shown in Fig. 6a, multiple self-healing iterations gave relatively high healing efficiency. The first round of healing showed an average of ~90% tensile

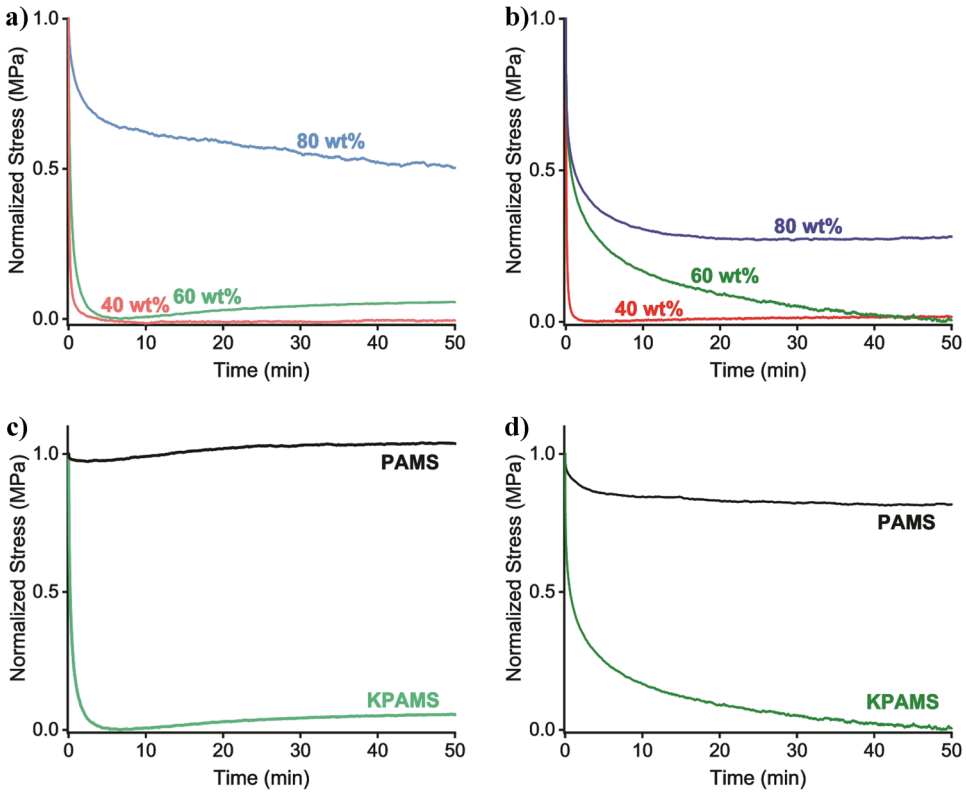

Fig. 5 Stress relaxation curves of **a** KPAMS-BDDE and **b** KPAMS-DGEBA. In both cases, increasing the KPAMS concentration results in faster stress relaxation as a result of increased dynamic bonding. Control groups without dynamic bond exchanges (PAMS) were also compared to **c** KPAMS-BDDE (60 wt%) and **d** KPAMS-DGEBA (60 wt%) to confirm the silanolate groups increase the rate of stress relaxation. All studies were performed at 110 °C with 1% axial strain

strength of the original sample. Stress–strain curves of multiple KPAMS-BDDE pristine samples in Fig. S10 help to show that the variation seen in the tensile tests after repeated self-healing cycles were within error. To confirm that any increase in variation in mechanical properties was not due to additional curing within the sample, DSC was used to show that the T_g of KPAMS-BDDE did not change before and after the self-healing process (Fig. S11). Although the soft thermosets seemed to be capable of some healing in ambient conditions (above T_g), heat was used to compare self-healing properties of the stiff materials for polymer welding. The modulus of the material was not changed with multiple heating cycles, as evident in Fig. 6a.

The 60 wt% formulation of KPAMS-DGEBA was also evaluated for comparison to the stiff material. Figure 6b shows that, despite miscibility issues between KPAMS and DGEBA, this stiff adaptable network still demonstrated self-healing capabilities. However, the stiff thermoset did not heal as well as the soft material when the same healing conditions were used. Although not as efficient as the KPAMS-BDDE material, the 60 wt% DGEBA was able to self-heal through multiple cycles. While time, temperature, and pressure could be adjusted to optimize self-healing of each of the materials separately, this was outside the scope of the current work. By using consistent parameters for both KPAMS-BDDE and KPAMS-DGEBA, the same conditions could be used for welding the different materials together.

3.3.3 Welding dissimilar materials

As previously mentioned, bonding dissimilar materials is a major challenge across many industries. Yet, welding is desirable for polymeric materials because low surface energy inhibits strong bonding from adhesives [64–66], and mechanical fasteners can diminish structural integrity [67]. Polymer welding typically requires methods like using solvents or heat for the interpenetration of linear polymers [68, 69]. Therefore, welding has traditionally been mostly limited to thermoplastics, which can still be difficult with incompatible materials [29, 30]. Here, by incorporating silanolate groups for dynamic bonding, different thermosets containing compatible chemistry for siloxane equilibration can be welded together. Figure 7 shows the 60 wt% BDDE welded to the 60 wt% DGEBA material. The samples were welded using the same parameters implemented for self-healing studies. As the stress–strain curves indicate, the soft epoxy, with a Young's modulus of 18 MPa, is bonded to a stiff thermoset with a modulus of 1.1 GPa. In this lap shear configuration, the bonding strength was limited to the strength of the soft material, indicating interfacial welding of the two materials. This capability offers a solution to many applications that could benefit from robust bonding between soft and stiff materials and composites.

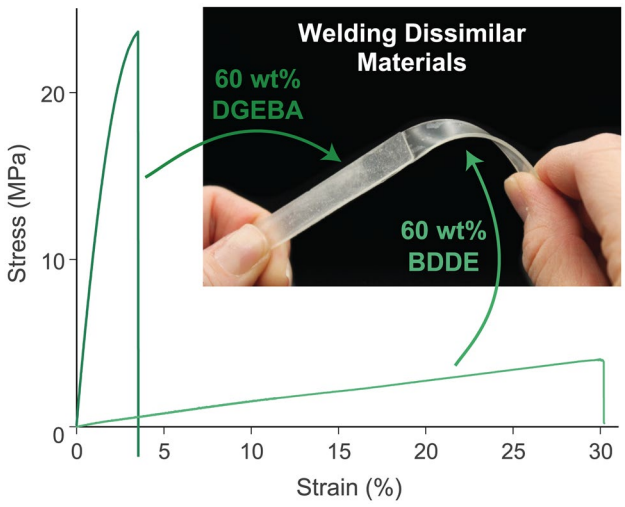

Fig. 7 Epoxy networks containing dynamic bonds allow polymer welding of dissimilar thermosets. Representative stress–strain curves of the stiff and soft adaptable networks show the two materials welded together have very different mechanical properties

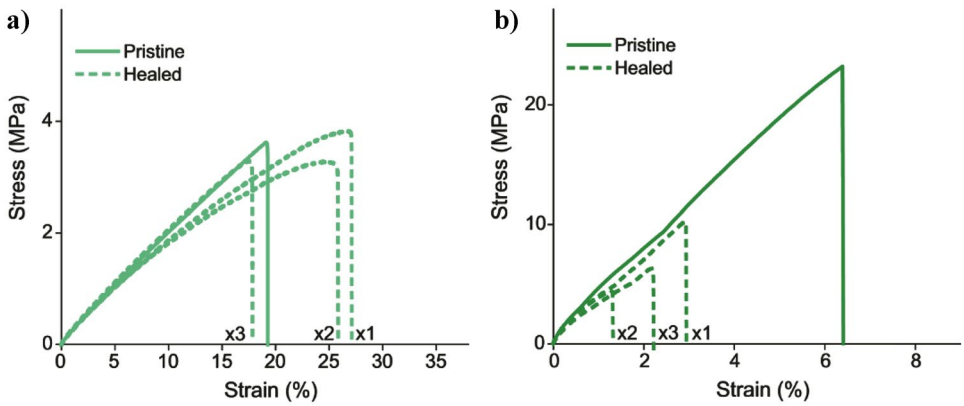

Fig. 6 Stress–strain curves comparing pristine samples with multiple cycles of self-healing for **a** 60 wt% BDDE (soft) and **b** 60 wt% DGEBA (stiff) adaptable networks. Both soft and stiff adaptable networks used the same conditions (110 °C, 45 min, 5 MPa) to heal dogbone specimens for tensile testing

4 Conclusion

This work encompasses a systematic study to evaluate the structure–property relationships of soft and stiff epoxy adaptable networks. Two separate adaptable networks were synthesized by combining a diepoxide crosslinker with a silanolate-functionalized oligosiloxane. The concentration of the diepoxide monomers was varied to study the effect of crosslinker content on the properties of different thermosets. The flexible BDDE monomer exhibited an optimal composition at 60 wt% with an increased T_g value (11 °C), tensile strength (3.9 MPa) and strain at break (29%). Stiff adaptable networks were prepared with the rigid monomer DGEBA, where mechanical properties had a more linear correlation with the amount of crosslinker added. The mechanical properties of the KPAMS-DGEBA materials could be tailored by altering the ratios of the starting materials, e.g., high tensile strength (51 MPa) with more crosslinker or high strain at break (32%) with less. However, the KPAMS-DGEBA materials with lower concentrations of DGEBA showed evidence of immiscibility. With both adaptable networks, the T_g and modulus were dependent on the degree of crosslinking, which was altered by stoichiometric ratios between epoxide and amine groups in each of the formulations. The different materials also showed self-healing capabilities, as evidenced by stress relaxation and self-healing studies. Using similar healing conditions, the soft KPAMS-BDDE adaptable network was welded to the stiff KPAMS-DGEBA adaptable network. By incorporating compatible dynamic components into separate materials, we demonstrated that dissimilar thermosets can be welded together. This ability to tune thermal and mechanical properties makes these sustainable materials particularly well-suited for a range of applications such as welding into laminates for biomedical, aerospace, or automotive industries.

Supplementary Information The online version contains supplementary material available at https://doi.org/10.1007/s42114-022-00558-4.

Acknowledgements This research was performed while A. A. Putnam-Neeb, A. M. Hubbard, and D. P. Street held National Research Council (NRC) Research Associateship awards at the Air Force Research Laboratory. The authors thank Arthur Safriet and the machine shop at AFRL Materials and Manufacturing Directorate for support in machining dogbone molds.

Funding This research was funded with the support by the Air Force Research Laboratory-Materials and Manufacturing Directorate as well as the Air Force Office of Scientific Research under grant number 22RXCOR014.

Declarations

Competing interests The authors declare no competing interests.

References

1. Wang B, Zhang Z, Pei Z et al (2020) Current progress on the 3D printing of thermosets. Adv Compos Hybrid Mater 3:462–472. https://doi.org/10.1007/s42114-020-00183-z
2. Chen Y, Wang Y, Su T et al (2019) Self-healing polymer composites based on hydrogen bond reinforced with graphene oxide. ES Mater Manuf 4:31–37. https://doi.org/10.30919/esmm5f214
3. Feng Y, Li Y, Ye X et al (2022) Synthesis and characterization of 2,5-furandicarboxylic acid poly(butanediol sebacate-butanediol) terephthalate (PBSeT) segment copolyesters with excellent water vapor barrier and good mechanical properties. J Mater Sci 57:10997–11012. https://doi.org/10.1007/s10853-022-07269-7
4. Cao Y, Weng M, Mahmoud MH et al (2022) Flame-retardant and leakage-proof phase change composites based on MXene/polyimide aerogels toward solar thermal energy harvesting. Adv Compos Hybrid Mater. https://doi.org/10.1007/s42114-022-00504-4
5. Mooss VA, Vijayakumar V, Kurungot S, Athawale AA (2021) Interconnected polyaniline nanostructures: enhanced interface for better supercapacitance retention. Polymer 212:123169. https://doi.org/10.1016/j.polymer.2020.123169
6. Li H, Huang W, Qiu B et al (2022) Effective removal of proteins and polysaccharides from biotreated wastewater by polyaniline composites. Adv Compos Hybrid Mater. https://doi.org/10.1007/s42114-022-00508-0
7. Alipoori S, Rouhi H, Linn E et al (2021) Polymer-based devices and remediation strategies for emerging contaminants in water. ACS Appl Polym Mater 3:549–577. https://doi.org/10.1021/acsapm.0c01171
8. Naseri M, Fotouhi L, Ehsani A (2018) Recent progress in the development of conducting polymer-based nanocomposites for electrochemical biosensors applications: a mini-review. Chem Rec 18:599–618. https://doi.org/10.1002/tcr.201700101
9. Ma Z, Li S, Wang H et al (2019) Advanced electronic skin devices for healthcare applications. J Mater Chem B 7:173–197. https://doi.org/10.1039/C8TB02862A
10. Lu Y, Liu Z, Yan H et al (2019) Ultrastretchable conductive polymer complex as a strain sensor with a repeatable autonomous self-healing ability. ACS Appl Mater Interfaces 11:20453–20464. https://doi.org/10.1021/acsami.9b05464
11. Jayalakshmi CG, Inamdar A, Anand A, Kandasubramanian B (2018) Polymer matrix composites as broadband radar absorbing structures for stealth aircrafts. J Appl Polym Sci. https://doi.org/10.1002/app.47241
12. Wu W, Li Z, Lin G et al (2022) Additive manufacturing of continuous BF-reinforced PES composite material and mechanical and wear

properties evaluation. J Mater Sci 57:12903–12915. https://doi.org/10.1007/s10853-022-07425-z
13. Odian G (2004) Principles of polymerization, 4th edn. John Wiley & Sons Inc, Hoboken, NJ, USA
14. Scheutz GM, Lessard JJ, Sims MB, Sumerlin BS (2019) Adaptable crosslinks in polymeric materials: resolving the intersection of thermoplastics and thermosets. J Am Chem Soc 141:16181–16196. https://doi.org/10.1021/jacs.9b07922
15. Kloxin CJ, Bowman CN (2013) Covalent adaptable networks: smart, reconfigurable and responsive network systems. Chem Soc Rev 42:7161–7173. https://doi.org/10.1039/c3cs60046g
16. García F, Smulders MMJ (2016) Dynamic covalent polymers. J Polym Sci Part A Polym Chem 54:3551–3577. https://doi.org/10.1002/pola.28260
17. Chakma P, Konkolewicz D (2019) Dynamic covalent bonds in polymeric materials. Angew Chem Int Ed 58:9682–9695. https://doi.org/10.1002/anie.201813525
18. Roy N, Bruchmann B, Lehn J-M (2015) DYNAMERS: dynamic polymers as self-healing materials. Chem Soc Rev 44:3786–3807. https://doi.org/10.1039/C5CS00194C
19. Song T, Jiang B, Li Y et al (2021) Self-healing materials: a review of recent developments. ES Mater Manuf 14:1–19. https://doi.org/10.30919/esmm5f465
20. Wang Y, Huang X, Zhang X (2021) Ultrarobust, tough and highly stretchable self-healing materials based on cartilage-inspired noncovalent assembly nanostructure. Nat Commun 12:1291. https://doi.org/10.1038/s41467-021-21577-7
21. Sun D, Yan J, Ma X et al (2021) Tribological investigation of self-healing composites containing metal/polymer microcapsules. ES Mater Manuf 14:59–72. https://doi.org/10.30919/esmm5f469
22. Zheng P, McCarthy TJ (2010) Rediscovering silicones: molecularly smooth, low surface energy, unfilled, UV/Vis-transparent, extremely cross-linked, thermally stable, hard, elastic PDMS. Langmuir 26:18585–18590. https://doi.org/10.1021/LA104065E
23. Zheng P, McCarthy TJ (2012) A surprise from 1954: siloxane equilibration is a simple, robust, and obvious polymer self-healing mechanism. J Am Chem Soc 134:2024–2027. https://doi.org/10.1021/ja2113257
24. Zhao J, Xu R, Luo G et al (2016) A self-healing, re-moldable and biocompatible crosslinked polysiloxane elastomer. J Mater Chem B 4:982–989. https://doi.org/10.1039/c5tb02036k
25. Keller MW, White SR, Sottos NR (2007) A self-healing poly(dimethyl siloxane) elastomer. Adv Funct Mater 17:2399–2404. https://doi.org/10.1002/ADFM.200700086
26. Yang H, Yu K, Mu X et al (2016) Molecular dynamics studying on welding behavior in thermosetting polymers due to bond exchange reactions. RSC Adv 6:22476–22487. https://doi.org/10.1039/c5ra26128g
27. Yu K, Shi Q, Li H et al (2016) Interfacial welding of dynamic covalent network polymers. J Mech Phys Solids 94:1–17. https://doi.org/10.1016/j.jmps.2016.03.009
28. Stukalin EB, Cai LH, Kumar NA et al (2013) Self-healing of unentangled polymer networks with reversible bonds. Macromolecules 46:7525–7541. https://doi.org/10.1021/MA401111N
29. Röttger M, Domenech T, van der Weegen R et al (2017) High-performance vitrimers from commodity thermoplastics through dioxaborolane metathesis. Science 356:62–65. https://doi.org/10.1126/science.aah5281
30. Hu K, Wei T, Li H et al (2019) Interfacial broadening kinetics between a network and a linear polymer and their composites prepared by melt blending. Macromolecules 52:9759–9765. https://doi.org/10.1021/acs.macromol.9b02114
31. Li X, Yu R, Zhao T et al (2018) A self-healing polysiloxane elastomer based on siloxane equilibration synthesized through amino-ene Michael addition reaction. Eur Polym J 108:399–405. https://doi.org/10.1016/j.eurpolymj.2018.09.021
32. de Buyl F (2001) Silicone sealants and structural adhesives. Int J Adhes Adhes 21:411–422. https://doi.org/10.1016/S0143-7496(01)00018-5
33. Schmolke W, Perner N, Seiffert S (2015) Dynamically crosslinked polydimethylsiloxane networks with ambienterature self-healing. Macromolecules 48:8781–8788. https://doi.org/10.1021/acs.macromol.5b01666
34. Wang DP, Zhao ZH, Li CH, Zuo JL (2019) An ultrafast self-healing polydimethylsiloxane elastomer with persistent sealing performance. Mater Chem Front 3:1411–1421. https://doi.org/10.1039/c9qm00115h
35. Sun S, Fei G, Wang X et al (2021) Covalent adaptable networks of polydimethylsiloxane elastomer for selective laser sintering 3D printing. Chem Eng J 412:128675. https://doi.org/10.1016/j.cej.2021.128675
36. Wu X, Yang X, Yu R et al (2018) A facile access to stiff epoxy vitrimers with excellent mechanical properties: via siloxane equilibration. J Mater Chem A 6:10184–10188. https://doi.org/10.1039/c8ta02102c
37. Treloar LRG (1973) The elasticity and related properties of rubbers. Rep Prog Phys 36:755–826
38. Zhou Z, Su X, Liu J, Liu R (2020) Synthesis of vanillin-based polyimine vitrimers with excellent reprocessability, fast chemical degradability, and adhesion. ACS Appl Polym Mater 2:5716–5725. https://doi.org/10.1021/acsapm.0c01008
39. ASTM International (2015) ASTM D638–14 standard test method for tensile properties of plastics. ASTM International, West Conshohocken, PA
40. Zaquen N, Rubens M, Corrigan N et al (2020) Polymer synthesis in continuous flow reactors. Prog Polym Sci 107:101256. https://doi.org/10.1016/j.progpolymsci.2020.101256
41. Reis MH, Leibfarth FA, Pitet LM (2020) Polymerizations in continuous flow: recent advances in the synthesis of diverse polymeric materials. ACS Macro Lett 9:123–133. https://doi.org/10.1021/acsmacrolett.9b00933
42. Plutschack MB, Pieber B, Gilmore K, Seeberger PH (2017) The Hitchhiker's guide to flow chemistry. Chem Rev 117:11796–11893. https://doi.org/10.1021/acs.chemrev.7b00183
43. de Boulle K, Glogau R, Kono T et al (2013) A review of the metabolism of 1,4-butanediol diglycidyl ether-crosslinked hyaluronic acid dermal fillers. Dermatol Surg 39:1758–1766. https://doi.org/10.1111/dsu.12301
44. Hermanson GT (2013) PEGylation and synthetic polymer modification. In: Bioconjugate Techniques. Elsevier, pp 787–838
45. Ebewele RO (2000) Polymer science and technology. CRC Press, Boca Raton
46. Crawford E, Lesser AJ (1998) The effect of network architecture on the thermal and mechanical behavior of epoxy resins. J Polym Sci Part B: Polym Phys 36:1371–1382. https://doi.org/10.1002/(SICI)1099-0488(199806)36:8%3c1371::AID-POLB11%3e3.0.CO;2-4
47. Crawford ED, Lesser AJ (1999) Brittle to ductile: fracture toughness mapping on controlled epoxy networks. Polym Eng Sci 39:385–392. https://doi.org/10.1002/pen.11425
48. Petersen HN, F. Minty R, Thomason JL et al (2019) The amine:epoxide ratio at the interface of a glass fibre/epoxy matrix system and its influence on the interfacial shear strength. Compos Interfaces 26:493–505. https://doi.org/10.1080/09276440.2018.1511107
49. Odagiri N, Shirasu K, Kawagoe Y et al (2021) Amine/epoxy stoichiometric ratio dependence of crosslinked structure and ductility in amine-cured epoxy thermosetting resins. J Appl Polym Sci. https://doi.org/10.1002/app.50542
50. Yang Y, Xu Y, Ji Y, Wei Y (2021) Functional epoxy vitrimers and composites. Prog Mater Sci. https://doi.org/10.1016/j.pmatsci.2020.100710
51. Yang X, Huang W, Yu Y (2012) Epoxy toughening using low viscosity liquid diglycidyl ether of ethoxylated bisphenol-A. J Appl Polym Sci 123:1913–1921. https://doi.org/10.1002/app.34677

52. Bagheri R, Marouf BT, Pearson RA (2009) Rubber-toughened epoxies: a critical review. Polym Rev 49:201–225. https://doi.org/10.1080/15583720903048227
53. Rosetti Y, Alcouffe P, Pascault JP et al (2018) Polyether sulfone-based epoxy toughening: From micro- to nano-phase separation via PES end-chain modification and process engineering. Materials. https://doi.org/10.3390/ma11101960
54. Fernandez B, Arbelaiz A, Diaz E, Mondragon I (2004) Influence of polyethersulfone modification of a tetrafunctional epoxy matrix on the fracture behavior of composite laminates based on woven carbon fibers. Polym Compos 25:480–488. https://doi.org/10.1002/pc.20041
55. Jiang M, Liu Y, Cheng C et al (2018) Enhanced mechanical and thermal properties of monocomponent high performance epoxy resin by blending with hydroxyl terminated polyethersulfone. Polym Test 69:302–309. https://doi.org/10.1016/j.polymertesting.2018.05.039
56. Cho JB, Hwang JW, Cho K et al (1993) Effects of morphology on toughening of tetrafunctional epoxy resins with poly(ether imide). Polymer 34:4832–4836
57. Chen Z, Luo J, Huang Z et al (2020) Synergistic toughen epoxy resin by incorporation of polyetherimide and amino groups grafted MWCNTs. Compos Commun 21:100377. https://doi.org/10.1016/j.coco.2020.100377
58. Ma H, Aravand MA, Falzon BG (2019) Phase morphology and mechanical properties of polyetherimide modified epoxy resins: A comparative study. Polymer 179:121640. https://doi.org/10.1016/J.POLYMER.2019.121640
59. Huang J, Nie X (2016) A simple and novel method to design flexible and transparent epoxy resin with tunable mechanical properties. Polym Int 65:835–840. https://doi.org/10.1002/pi.5144
60. Ligon-Auer SC, Schwentenwein M, Gorsche C et al (2016) Toughening of photo-curable polymer networks: a review. Polym Chem 7:257. https://doi.org/10.1039/c5py01631b
61. Bhuniya S, Adhikari B (2003) Toughening of epoxy resins by hydroxy-terminated, silicon-modified polyurethane oligomers. J Appl Polym Sci 90:1497–1506. https://doi.org/10.1002/app.12666
62. Lin ST, Huang SK (1996) Synthesis and impact properties of siloxane-DGEBA epoxy copolymers. J Polym Sci Part A: Polym Chem 34:1907–1922. https://doi.org/10.1002/(SICI)1099-0518(19960730)34:10%3c1907::AID-POLA8%3e3.0.CO;2-L
63. Othman MBH, Ahmad Z, Kua HS et al (2016) Incorporation of hydroxyl terminated polydimethylsiloxane into DGEBA epoxy resins via condensation of hydroxyl groups: preliminary approach. Walailak J Sci Tech 13:923–930
64. Sonnenschein MF, Webb SP, Cieslinski RC, Wendt BL (2007) Poly(acrylate/epoxy) Hybrid adhesives for low-surface-energy plastic adhesion. J Polym Sci Part A: Polym Chem 45:989–998. https://doi.org/10.1002/pola.21843
65. Sonnenschein MF, Webb SP, Wendt BL (2008) Poly(acrylate/siloxane) hybrid adhesives for polymers with low surface energy. Int J Adhes Adhes 28:126–134. https://doi.org/10.1016/J.IJADHADH.2007.07.001
66. Putnam AA, Wilker JJ (2021) Changing polymer catechol content to generate adhesives for high versus low energy surfaces. Soft Matter 17:1999–2009. https://doi.org/10.1039/d0sm01944e
67. Kinloch AJ (1987) Adhesion and adhesives: science and technology. Springer, New York
68. Ebnesajjad S (2009) Solvent cementing of plastics. In: Adhesives Technology Handbook, Second Edition. William Andrew Publishing, pp 209–229
69. Dodin MG (1981) Welding mechanisms of plastics: a review. J Adhes 12:99–111. https://doi.org/10.1080/00218468108071192